PHYSICAL REVIEW B VOLUME 57, NUMBER 10 1 MARCH 1998-II

Nonlocal supercurrent in mesoscopic Josephson junctions

J. P. Heida, B. J. van Wees, and T. M. Klapwijk
Department of Applied Physics and Material Science Centre, University of Groningen, Nijenborgh 4, 9747 AG Groningen, The Netherlands

G. Borghs
Interuniversity Microelectronics Centre, Kapeldreef 75, B-3030, Leuven, Belgium

(Received 29 May 1997)

We demonstrate that in a mesoscopic, fully phase coherent, superconductor–two-dimensional-electron-gas–superconductor structure the period of the critical current versus flux through the junction is h/e, i.e., twice the superconducting flux quantum. Using a heuristic approach we argue that the observations point to a nonlocal supercurrent density. The particles carrying the supercurrent sense the superconductor phase, which is spatially modulated by the magnetic field, along the entire electrode. [S0163-1829(98)50510-3]

A local description is not sufficient to describe the electronic properties of mesoscopic samples. Instead it is essential to take quantum mechanical interference extending over the phase coherent area into account. A prime example is that Ohm's law, the local relation between current density J and electric field E, has to be replaced by a *nonlocal* one:

$$\mathbf{J}(\mathbf{r}) = \int d\mathbf{r}' \underline{\sigma}(\mathbf{r},\mathbf{r}') \cdot \mathbf{E}(\mathbf{r}'), \tag{1}$$

where $\underline{\sigma}(\mathbf{r},\mathbf{r}')$ is a conductivity tensor.[1] Is there in analogy a *nonlocal* dependence of the supercurrent density on the phase difference between the electrodes in a mesoscopic Josephson junction? That is to say, is the supercurrent density at position x_1 on electrode 1 built up from contributions of the entire opposite electrode 2 (see Fig. 1) given by

$$\mathbf{J}_s(x_1) = \int dx_2 f(\phi(x_1,x_2)), \tag{2}$$

where f is a function of the superconductor phase difference $\phi(x_1,x_2)$ between x_1 and x_2, contrasting the *local* relation $\mathbf{J}_s(x_1) = f(\phi(x_1))$ for tunneling Josephson junctions?

In this paper we address this issue which is at the heart of ''mesoscopic supercurrents'' with a particularly suitable class of junctions. These are fully phase coherent planar superconductor–two-dimensional-electron-gas–superconductor junctions and have a comparable width W and length L, $l_\phi > L, W$ (l_ϕ is the phase coherence length). So far, experimentalists[2] have focused on the supercurrent magnitude, temperature dependence, supercurrent fluctuations, and possible supercurrent quantization in mesoscopic Josephson junctions. These properties were explicitly treated in a number of theoretical papers.[3] The concept of Andreev reflection,[4] which mediates the conversion of current in a normal metal to a Cooper pair current in a connected superconductor has been the starting point in all these theories as the microscopic origin of the supercurrent. It is generally accepted that coherent Andreev reflections and interference of electrons and holes lead to bound states which carry a supercurrent. The phase difference γ between the superconductors has a crucial influence on the properties of these bound states such as the energy $E(\gamma)$, and the amount of supercurrent $I_s(\gamma)$ carried.

Most likely the answer to the question raised above is affirmative since the particles carrying the supercurrent in a mesoscopic Josephson junction probe the superconductor phase at different positions, unlike tunneling Josephson junctions where the supercurrent density flows directly to the opposite electrode. Because a magnetic field modulates the superconductor phase, this nonlocality will have its repercussions on the supercurrent in a magnetic field.

In a magnetic field, characterized by a vector potential $\mathbf{A}$, the gauge-invariant phase difference γ between points x_1 and x_2 (see Fig. 1) is

$$\gamma = [\phi_2(x_2) - \phi_1(x_1)] - \frac{2\pi}{\Phi_0} \int_{(x_1,0)}^{(x_2,L)} \vec{A} d\vec{l}, \tag{3}$$

where $\Phi_0 = h/2e$ is the superconducting flux quantum. For a local supercurrent density flowing from x_1 on electrode 1 to a specific x_2 on electrode 2 (for tunnel junctions one takes $x_1 = x_2$) the net result for the experimentally accessible quantity, the critical current at a given field $B\hat{z}$, is

$$I_c = \max\left[\int_0^W J_s(\gamma(x)) dx \right] = I_{c0} \left| \frac{\sin(\pi\Phi/\Phi_0)}{\pi\Phi/\Phi_0} \right|, \tag{4}$$

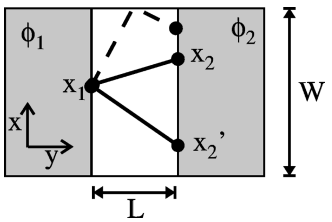

FIG. 1. Josephson junction showing lengths and directions used in the text. Electrode 1 and 2 have macroscopic phases ϕ_1 and ϕ_2, respectively. Supercurrent can flow from x_1 at electrode 1 to any x_2 at electrode 2, and possibly via the sidewalls (dashed line).

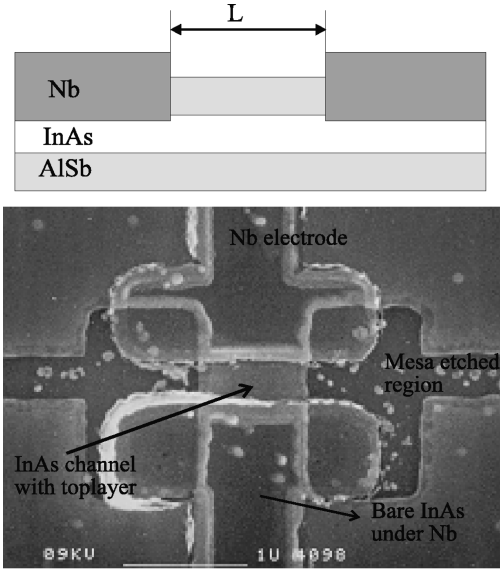

FIG. 2. Top: schematic cross section of a S-2DEG-S junction. Bottom: Scanning electron microscopy photo of the junction.

where $\Phi = BWL$,[5] the flux penetrating the junction area. This so-called Fraunhofer diffraction pattern with period Φ_0 was first observed by Rowell.[6] It arises because the local supercurrent density flowing in different parts of the sample has a position-dependent magnitude and sign, leading to (partial) cancellation in the net supercurrent of the entire sample.

For the mesoscopic junctions under study where $W \approx L$, particles can sense the entire junction and the supercurrent density at x_1 is built up from contributions over the entire sample. We thus expect a different magnetic field dependence of the supercurrent.

A schematic figure and a scanning electron micrograph of the sample are reproduced in Fig. 2. As coupling material between the Nb electrodes a two-dimensional electron gas (2DEG) in a 15-nm-thick InAs quantum well (QW) between AlSb barriers is used. To produce the sample first the mesa-etch pattern is written in PMMA using electron beam lithography (EBL). This pattern is transferred to the heterostructure by wet etching of the AlSb top layer and the InAs quantum well.[7,8] Secondly, the electrode pattern is defined in PMMA with EBL and the AlSb top layer is removed by chemical etching to expose the InAs QW. Finally the sample is loaded in a UHV chamber where the InAs QW surface is cleaned with a 500 eV Ar-ion bombardment prior to deposition of 70-nm-thick Nb electrodes.

The ion bombardment modifies the region under the Nb contact. Locally the bombardment reduces the electron mean free path to approximately 10 nm and induces a high electron density. However, this treatment is necessary to create a transparent Nb-2DEG interface.[9] An important consequence of the Ar-ion bombardment is that the Andreev reflection taking place at the 2DEG-superconductor interface is of diffusive nature. Whereas for Andreev reflection from a specular interface, the hole is retroreflected and has the same wave vector as the incoming electron from which it originates, the reflected hole from a diffusive interface has partial waves in all directions.[7] Since the supercurrent is carried by bound states formed by multiple Andreev reflections, this effect promotes the nonlocality of the supercurrent density in the devices studied.

TABLE I. Parameters of the junctions.

Sample	length (μm)	I_c (nA)	R_n (Ω)	Φ_{period} (mT)
A	0.32	131	327	4.2
B	0.47	236	324	3.7
C	0.63	53	381	3.5
D	0.78	98	431	3.2

Four junctions were prepared on the same chip of InAs in the same production batch. Their mesa-etch width is $W = 0.7$ μm. The Nb-2DEG contact is made in the dark region in Fig. 2 (indicated as bare InAs under Nb). The interelectrode distance L is the length of the channel between these regions in the upper and lower part of the scanning electron microscopy picture, it ranges from 0.32 to 0.78 μm. The channels are covered with an AlSb top layer to ensure a high mobility, ballistic channel.

The details of the characterization will be discussed elsewhere,[11,8] here we present the main results. The samples have an electron density $n_s = 2.1 \times 10^{16}$ m^{-2} as obtained from Shubnikov–de Haas measurements of the actual sample, and an electron mean free path of at least 1 μm. Thus the samples have a ballistic channel, as supported by the low magnetic field behavior of their resistance which is dominated by magnetic depopulation of the subbands.[10] The measured resistances (see Table I) are higher than the Sharvin resistance $R_{Sh} = (h/2e^2)\pi/k_F W = 160$ Ω. This is due to scattering at the interfaces, and possibly some remnant scattering in the channel itself. As mentioned, both the width and the length of the samples are smaller than the phase coherence length l_ϕ which is bounded by the inelastic scattering length $l_{in} \approx 10$ μm.[12] At the low temperatures used it is also smaller than the thermal coherence length $\xi_T = \hbar v_F / 2\pi k_B T \approx 15$ μm (at 0.1 K). Moreover, the junction dimensions are comparable to the superconducting coherence length $\xi_0 = \hbar v_F / 2\Delta \approx 0.5$ μm (with $\Delta = 1.1$ meV), so that they are in between the long ($L \gg \xi_0$) and short ($L \ll \xi_0$) limit.

Summarizing, the sample is a ballistic channel bounded by high transparancy superconducting electrodes on top of a disordered InAs region where diffusive Andreev reflection takes place, and electrons can travel phase coherently between the electrodes. Therefore the junctions can carry a supercurrent.

The current voltage characteristics of all four samples show a supercurrent; its optimal magnitude is tabulated in Table I along with other parameters of the junction. Its magnitude is an order of magnitude smaller than expected for both diffusive and ballistic junctions close to the short limit having high transparancy interfaces.[13,14] Also the critical current does not scale with the electrode separation. These aspects, along with the current-voltage characteristics, will be covered elsewhere. Here we focus on the influence of the magnetic field on the zero voltage supercurrent at the lowest temperature. In Fig. 3 the supercurrent versus magnetic field is shown up to fields where the supercurrent can be obtained directly from a well defined switching current in the current

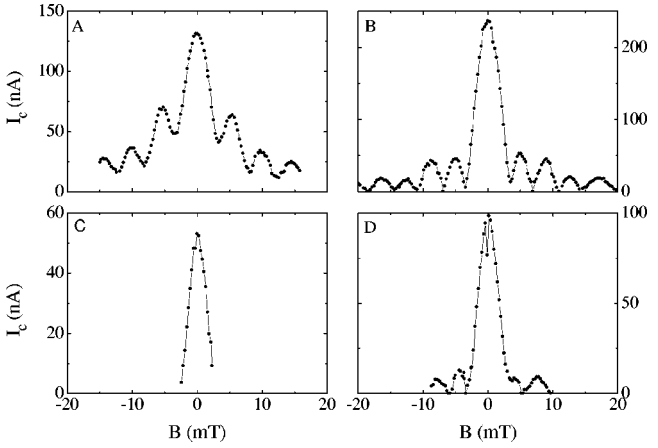

FIG. 3. Critical currents of junctions A,B,C, and D versus magnetic field at $T=0.1$ K.

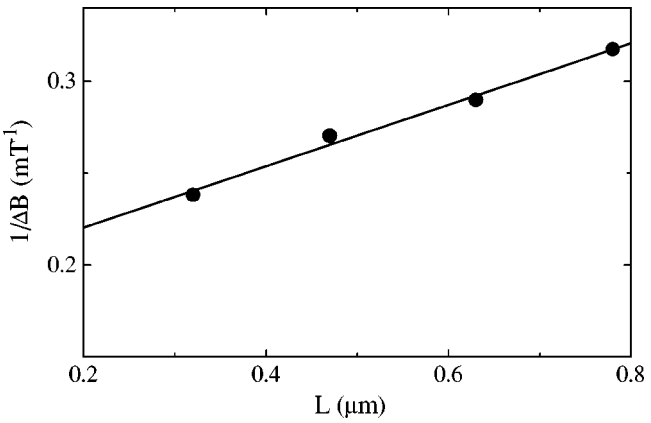

FIG. 4. Inverse of measured period ΔB versus junction length L.

voltage characteristic. All four junctions show a clear maximum in the supercurrent and its oscillatory decay. However the functional dependence is not the Fraunhofer pattern expected from standard theory.

The periodicity of the supercurrent in magnetic field as seen in Fig. 3 is confirmed by measurements of the differential resistance versus magnetic field. The supercurrent modifies the differential resistance and this provides a sensitive technique to identify the presence of small supercurrents.[15] In this way more periods are traced from which the periodicities, reported in Table I, are acquired with higher accuracy. These are to be converted to the amount of flux actually penetrating the junction area.

In addition to the flux penetrating the region $W\times L$,[5] due to the screening currents in the electrode, there is a considerable amount of flux expelled from the Nb electrodes which are pushed through this area.[16] This ''flux crowding'' effect has hindered definite statements on the amount of flux penetrating the junction area in previous experiments. Here we isolate this contribution by choosing samples of different length. It is taken into account by adding an extra length L_M to the junction length L. In the junction geometry under study this is allowed because the Nb electrodes are considerably wider than the InAs channel region. The flux Φ penetrating the junction will be:

$$\Phi=(L+L_M)WB, \tag{5}$$

so that for the periodicity ΔB:

$$\frac{1}{\Delta B}=\frac{1}{\Delta\Phi}W(L+L_M). \tag{6}$$

Thus the slope of a plot of the inverse magnetic field period versus the junction length yields the true period in flux $\Delta\Phi$ incorporating expelled flux from the superconducting electrodes. The contribution of the expelled flux, i.e., L_M, is acquired from the $1/\Delta B$ axis intercept. Figure 4 shows such a plot; the result is that $\Delta\Phi=4.2\times10^{-15}$ Wb. This value is $\approx 2\Phi_0$, thus the critical current vs magnetic field pattern period is *doubled* compared to Eq. (4). The extra length due to the screening currents L_M is 1.1 μm, 0.55 μm at each electrode of the junction, slightly more than expected from the SEM figure if half of the width of the Nb electrodes would determine L_M.

Thus neither the functional dependence nor the periodicity of Eq. (4) is reproduced. A local supercurrent density that is position dependent (so that it is not just a function of phase difference, but also of position) can cause a functional dependence of the supercurrent in a magnetic field deviating from Eq. (4). This goes along with a modified period that can be larger than Φ_0. For the mesoscopic samples discussed the functional dependence is not shared by all samples, yet the period in flux is. With any local supercurrent density it is highly coincidental that different functional dependencies go along with identical periods. Thus, in all likelihood, the data reflect an inherent phenomenon due to the mesoscopic nature of these samples.

We now proceed to present a heuristic approach using a quasiclassical description which reproduces the observed periodicity, and might help to achieve some more insight to the question at stake. For a sinusoidal current phase relation, and an equal contribution to $\mathbf{J}(x_1)$ of all paths $x_1\rightarrow x_2$, as suggested by the length independence of the supercurrent, Eq. (2) becomes

$$\mathbf{J}_s(x_1)=\int_0^W J_{s0}\sin[\gamma(x_1,x_2)]\mathrm{d}x_2. \tag{7}$$

The phase difference $\gamma(x_1,x_2)$ is easily obtained with the vector potential gauge $\mathbf{A}=Bx\hat{\mathbf{y}}$. Because the channel region in our devices is ballistic, the coupling between the electrodes is along a straight path. Therefore the integral term in Eq. (3) is the average value of the vector potential along this path, and

$$\gamma(x_1,x_2)=\frac{\pi}{W}\frac{\Phi}{\Phi_0}(x_1+x_2)+\gamma_0. \tag{8}$$

The net supercurrent for the entire junction now becomes

$$I_c=\max\left[\int_0^W \mathbf{J}(x_1)\mathrm{d}x_1\right]=I_{c0}\left(\frac{\sin(\frac{1}{2}\pi\Phi/\Phi_0)}{\frac{1}{2}\pi\Phi/\Phi_0}\right)^2. \tag{9}$$

This yields the correct experimental periodicity of $2\Phi_0$ with a minimum in the supercurrent each time an *even* number of

flux quanta penetrates the junction area.[17] The functional dependence of Eq. (9) resembles the experimental results of junction D where $W/L=0.9$. It differs from the observations for wider junctions like A and B ($W/L=$ 2.2 and 1.5, respectively) where the presumption that all paths contribute equally may not be fully satisfied. We have found that the introduction of a length dependence and angular distribution for the paths contributing to the supercurrent density to the model does not suffice to describe the experimental outcome. As indicated in Fig. 1, it is conceivable that supercurrent flows via (specular) reflection at the sidewalls. If we include this in the calculation, the periodicity remains $2\Phi_0$, and the sidelobes are higher; two features consistent with the observations. However, the inclusion of trajectories via the sidewalls yields supercurrent maxima at even flux quanta whereas we observe minima there. Also the sharpness of the data, prominent for example in Fig. 3, is surprising in view of the smoothness of the predictions of Eq. (9).

Thus the used heuristic approach with a nonlocal supercurrent density reproduces the observed periodicity $2\Phi_0$ and it is highly plausible that the mesoscopic nature of the samples is the origin of the observed periodicity. Clearly this calls for a more rigid, quantum mechanical treatment of the problem incorporating the diffusive nature of Andreev reflection at the interfaces. Such a treatment, hinted at by the presented data, would be a great opportunity to enhance our understanding of supercurrents in mesoscopic systems.

Concluding, we have demonstrated that in a new class of Josephson junctions which are fully phase coherent and have comparable width and length, the period of the critical current versus flux penetrating the junction, is $\approx h/e$, i.e., twice the superconducting flux quantum. It is plausible that this is caused by a nonlocal supercurrent density in these junctions.

We thank S. G. den Hartog and A. F. Morpurgo for stimulating discussions, and B. H. J. Wolfs for technical assistance. This work was financially supported by the Stichting voor Fundamenteel Onderzoek der Materie (FOM). B. J. van Wees acknowledges support from the Royal Dutch Academy of Sciences (KNAW).

[1] H. U. Baranger and A. D. Stone, Phys. Rev. B **40**, 8169 (1989).

[2] C. Nguyen, H. Kroemer, and E. L. Hu, Phys. Rev. Lett. **69**, 2847 (1992); H. Takayanagi, T. Akazaki, and J. Nitta, Phys. Rev. B **51**, 1374 (1995); Phys. Rev. Lett. **75**, 3533 (1995); H. Takayanagi, J. B. Hansen, and J. Nitta, Physica B **203**, 291 (1994); B. J. van Wees *et al.*, *ibid.* **203**, 285 (1994); L. C. Mur *et al.*, Phys. Rev. B **54**, R2327 (1996); A. Chrestin, T. Matsuyama, and U. Merkt, *ibid.* **55**, 8457 (1997).

[3] I. O. Kulik, Zh. Éksp. Teor. Fiz. **57**, 1745 (1969) [Sov. Phys. JETP **30**, 944 (1970)]; J. Bardeen and J. L. Johnson, Phys. Rev. B **5**, 72 (1972); A. Furusaki and M. Tsukada, Phys. Rev. B **43**, 10 164 (1991); C. W. J. Beenakker and H. van Houten, Phys. Rev. Lett. **66**, 3056 (1991); P. F. Bagwell, Phys. Rev. B **46**, 12 573 (1992); C. W. J. Beenakker, in *Transport Phenomena in Mesoscopic Systems*, Proceedings of the 14th Taniguchi Symposium, Shima, Japan, 1991, edited by H. Fukuyama and T. Ando (Springer, Berlin, 1992); U. Schüssler and R. Kümmel, Phys. Rev. B **47**, 2754 (1993); A. Chrestin, T. Matsuyama, and U. Merkt, *ibid.* **49**, 498 (1994).

[4] A. F. Andreev, Sov. Phys. JETP **19**, 1228 (1964).

[5] On a microscopic level the phase is transferred to the electrons and holes over $\xi_0 \ll L$, where ξ is a combination of the decay length in the material under the superconductor, and the coherence length in the superconductor. Consequently, the relevant area for the flux is $W(L+2\xi)\approx WL$. In the macroscopic description L is extended with $2\lambda_L$, the London penetration depth in both electrodes. This is strictly speaking only valid if $\xi > \lambda_L$.

[6] J. M. Rowell, Phys. Rev. Lett. **11**, 200 (1963).

[7] A. F. Morpurgo, B. J. van Wees, T. M. Klapwijk, and G. Borghs, Appl. Phys. Lett. **70**, 1435 (1997).

[8] A. F. Morpurgo *et al.*, Phys. Rev. Lett. **78**, 2636 (1997).

[9] P. H. C. Magnée *et al.*, Appl. Phys. Lett. **67**, 3569 (1995).

[10] C. W. J. Beenakker and H. van Houten, in *Solid State Physics* (Academic Press, New York, 1991), Vol. 44.

[11] J. P. Heida, Ph.D. thesis, University of Groningen, 1997.

[12] A. F. Morpurgo (private communication). This value is obtained from multiple Andreev reflections on the same material.

[13] I. O. Kulik and A. N. Omelyanchuk, Zh. Éksp. Teor. Fiz. Pis'ma Red. **21**, 216 (1975) [JETP Lett. **21**, 96 (1975)].

[14] I. O. Kulik and A. N. Omelyanchuk, Fiz. Nizk. Temp. **3**, 945 (1977) [Sov. J. Low Temp. Phys. **3**, 459 (1997)].

[15] V. Ambegaokar and B. I. Halperin, Phys. Rev. Lett. **22**, 1364 (1969).

[16] The Josephson current is negligible compared to the diamagnetic screening currents in the electrodes.

[17] In the wide ($W \gg l_\phi > L$) SNS and S-2DEG-S junctions studied so far, the local description sufficed because any appreciable deviation from $\gamma(x)$, $\delta\gamma = 2\pi(\Phi/\Phi_0)/(x_2 - x_1/W)$ requires $x_2 - x_1 \approx W$, which implies that $L_{path} \approx \sqrt{L^2+W^2} \gg l_\phi$, so that there is no supercurrent density at all for these paths. Consequently $\gamma(x_1, x_2) \approx \gamma(x_1)$ for wide junctions.